JOURNAL OF GEOPHYSICAL RESEARCH: SPACE PHYSICS, VOL. 118, 2756–2764, doi:10.1002/jgra.50299, 2013

Storm time meridional wind perturbations in the equatorial upper thermosphere

R. A. Haaser,[1] R. Davidson,[2] R. A. Heelis,[1] G. D. Earle,[2] S. Venkatraman,[1] and J. Klenzing[3]

Received 19 December 2012; revised 18 April 2013; accepted 24 April 2013; published 30 May 2013.

[1] We present observations from the Coupled Ion Neutral Dynamics Investigation (CINDI) of storm time meridional winds in the neutral atmosphere near the magnetic equator at 400 km altitude. Observations near the magnetic equator in the southern geographic hemisphere are dominated by energy inputs from the southern Polar Regions that produce south to north (equatorward) wind perturbations to accompany perturbations in the neutral density and temperature. In one exceptional case, when observations are made near midnight and the north magnetic pole rotates through the midnight sector, north to south (poleward) meridional wind perturbations are observed just south of the magnetic equator. Accompanying perturbations in the neutral density on the dayside and the nightside are consistent with observed increases in the ion temperature and inferred increases in the neutral temperature in accord with hydrostatic equilibrium.

Citation: Haaser, R. A., R. Davidson, R. A. Heelis, G. D. Earle, S. Venkatraman, and J. Klenzing (2013), Storm time meridional wind perturbations in the equatorial upper thermosphere, *J. Geophys. Res. Space Physics*, *118*, 2756–2764, doi:10.1002/jgra.50299.

1. Introduction

[2] Variations in high-latitude particle energy input and frictional heating in the thermosphere accompany changes in magnetic activity represented by indices such as AE and Dst. Many times, these changes are produced by a southward turning of the interplanetary magnetic field (IMF) [*Saiz et al*., 2008]. This localized heating at high latitudes is redistributed within a few hours over the entire global thermosphere, resulting in modifications in the temperature, composition, and winds [*Fuller-Rowell et al*., 1994].

[3] Measurements of storm time perturbations in the thermospheric density have been well documented from a variety of satellite-borne accelerometers [*Forbes et al*. 1996; *Sutton et al*., 2005; *Lühr et al*., 2012]. However, measurements of the thermospheric temperature are sparser and generally derived from density measurements with some assumptions about mass composition and hydrostatic equilibrium [*Weimer et al*., 2011; *Earle et al*., 2013]. Thermospheric wind measurements are also rather sparse, being restricted to specific locations near ground-based observatories [*Martinis et al*., 2001] or to lower altitudes where atmospheric emissions are sufficient to detect Doppler shifts from space [*Shepherd et al*., 1993; *Emmert et al*., 2001]. In most cases, while the average disturbed period winds have been assessed [*Wu et al*., 1994; *Fejer et al*., 2000], observations of thermospheric meridional winds near the equator during magnetic storms remain relatively few. Expectations for the storm time behavior of meridional winds are based on models of the coupled ionosphere and thermosphere driven by high latitude electric field and precipitating particle inputs [*Emery et al*., 1999; *Fuller-Rowell et al*., 2002; *Gardner and Schunk*, 2010]. These studies suggest that phase fronts in the thermosphere, produced by the high-latitude energy inputs, propagate toward the equator with velocities of 500–800 ms^{-1}. All these studies indicate a strong local time and longitude dependence in the response. Propagation away from high latitudes will be most effective in the midnight sector and in the longitude sector where the magnetic pole is tilted toward the midnight sector [*Fuller-Rowell et al*., 1994]. In this sector, the equatorward meridional winds may also propagate across the equator into the opposing hemisphere.

[4] In this work, we contrast the different behaviors of the equatorial thermosphere in response to storm time inputs observed during the rising phase of solar cycle 24. We examine five storm periods between August 2011 and March 2012, for which perturbations in the neutral atmosphere density and meridional neutral air wind are recorded by the Coupled Ion-Neutral Dynamics Investigation (CINDI) aboard the Communications/Navigation Outage Forecasting System (C/NOFS) satellite. These data are restricted to the perigee portions of the satellite orbit between 400 km and 410 km altitude where the ion temperature is measured by CINDI and used as a proxy for the neutral gas temperature.

2. Observations

[5] The measurements considered for this study are in situ observations made by instrumentation aboard the ACE, Wind,

[1]William B Hanson Center for Space Sciences, University of Texas at Dallas, Richardson, Texas, USA.
[2]Center for Space Science and Engineering, Virginia Tech, Blacksburg, Virginia, USA.
[3]Space Weather Laboratory/Code 674, Goddard Space Flight Center, Greenbelt, Maryland, USA.

Corresponding author: R. A. Haaser, William B Hanson Center for Space Sciences, University of Texas at Dallas, 800 W. Campbell Road, WT-15, Richardson, Texas 75080, USA. (rhaaser@utdallas.edu)

2169-9380/13/10.1002/jgra.50299

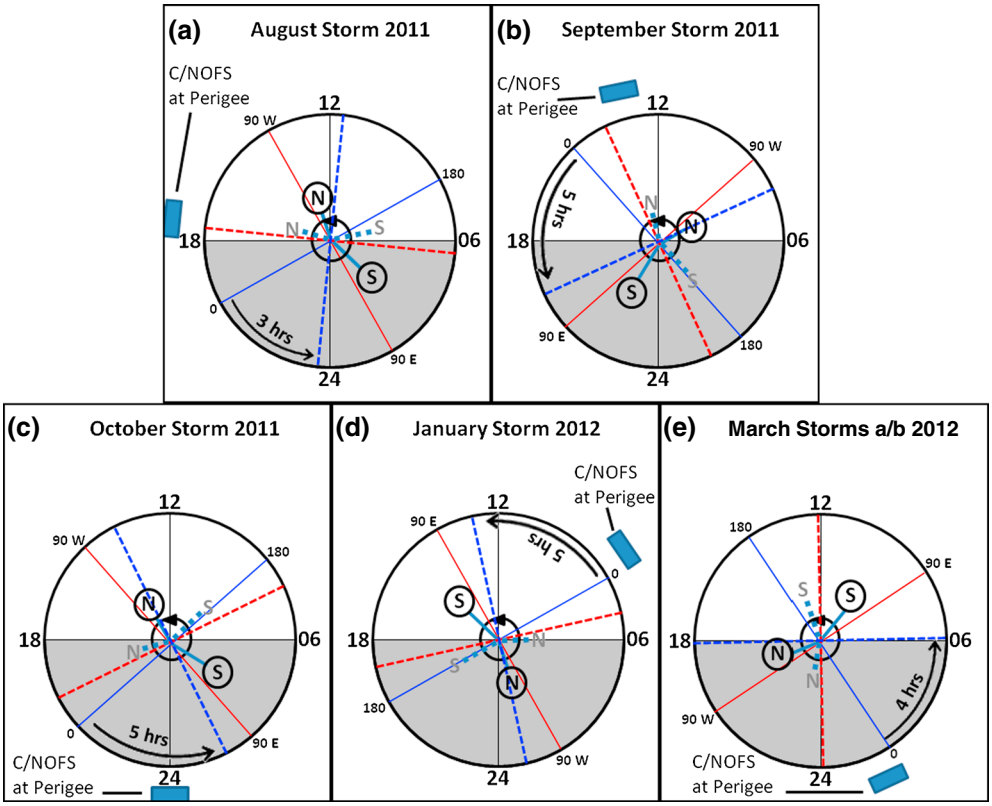

Figure 1. (a–e) For each event, the solid and dashed red and blue lines indicate the longitudes when the storm begins and when the storm is first observed, respectively. The blue rectangle represents the local time of the first storm time perturbation observations by C/NOFS. Also shown are the locations of the magnetic poles at the storm onset and their motion in the interval prior to the first perturbations observed near the equator.

and C/NOFS satellites. The ACE (Advanced Composition Explorer) and Global Geospace Science Wind spacecraft measure various geospace parameters, including the solar wind dynamic pressure and the Interplanetary Magnetic Field (IMF) [*von Rosenvinge et al.*, 1995; *Stone et al.*, 1998]. Data are obtained from the NASA Goddard OMNIWEB source, which includes a delay time to account for propagation to the anticipated location of the magnetopause. Also considered here is the Dst (Disturbance Storm Time) geomagnetic disturbance index. This index is used to characterize the magnetospheric response to the changes in the solar wind drivers and, in a qualitative sense, to normalize our expectations for the response of the low-latitude thermosphere [*Burton et al.*, 1975].

[6] The C/NOFS satellite was developed by the Air Force Research Laboratory to investigate the onset and evolution of plasma irregularities in the low-latitude ionosphere. CINDI is a NASA mission of opportunity comprising the Ion Velocity Meter (IVM) and Neutral Wind Meter (NWM) aboard the C/NOFS satellite to measure properties of the thermal ions and neutral gasses. The C/NOFS satellite was launched into a 13° inclination elliptical orbit with apogee near 800 km, and perigee near 400 km. The orbit period is about 96 min. The rotation of the line of apsides (connecting orbital perigee to apogee) and the local time precession of the orbit plane is such that all local times are sampled at perigee in approximately 2 months. In situ observations of neutral thermospheric number density and meridional neutral wind near 400 km are made from the cross-track sensor (CTS) in the NWM [*Haaser et al.*, 2010].

[7] In this work, we emphasize the different behaviors in the storm time meridional wind perturbations associated with the local time of the observation and the location of the magnetic poles during each of the five considered storm events occurring between August 2011 and March 2012. Observations are made at the satellite perigee near the geographic equator, and Figure 1 shows the local time of the observations and the configuration of the magnetic poles during each event. In each panel, a blue rectangle marks the perigee local time of the observations. For each event, there is a time delay of 3 to 5 h between the onset of the storm drivers, indicated by a southward turning of the IMF, and the response in the neutral atmosphere seen at the equator. The passage of the magnetic poles during this time period is also shown in each panel. The view is looking through the Earth from the North Pole. The North and South Poles for 2012 are located in geographic latitude and geographic longitude at 82.6°N, 276.2°E and 74.4°S, 125.8°E, respectively, calculated via International Geomagnetic Reference Field: the Eleventh Generation (IGRF-11) [*International Association of Geomagnetism and Aeronomy, Working Group V-MOD*, 2010].

[8] Figure 2 describes the storm drivers and the ionospheric and thermospheric response near the equator in a format that will be utilized for each of the events. Of the five

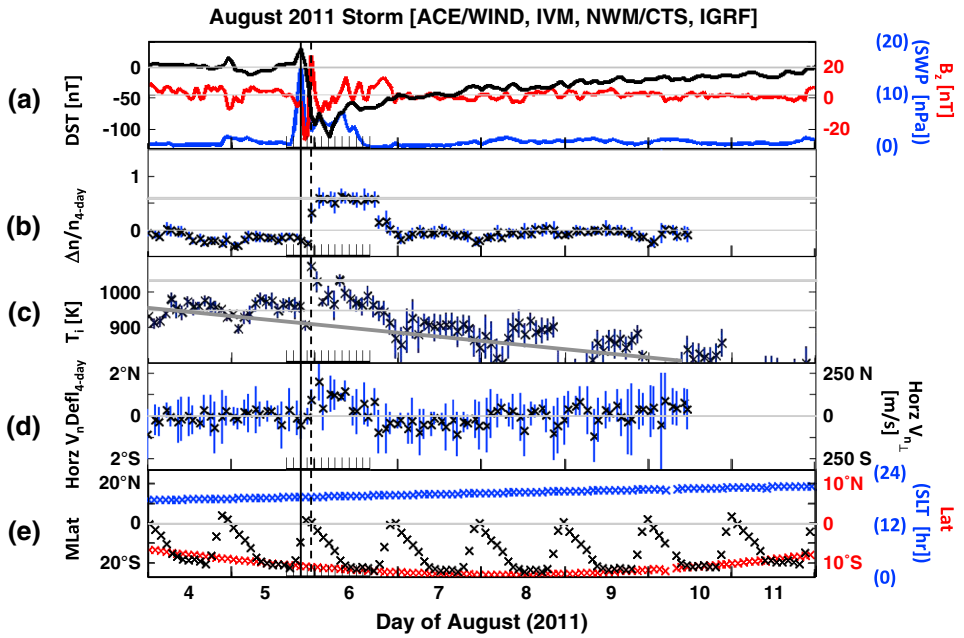

Figure 2. (a–e) August 2011 storm time responses in the upper thermosphere near the magnetic equator. Figure 2a shows the Dst index in black, the IMF Bz in red, and the solar wind dynamic pressure in blue. Figure 2b shows the fractional change in the observed ram pressure as a measure of the ambient neutral density change. The dark horizontal gray line indicates the maximum fractional increase. Figure 2c shows the change in the thermal ion temperature and Figure 2d the change in the meridional wind. All changes are determined from a 4 day running mean. A solid vertical line through all panels marks the storm onset, a dashed vertical line marks the apparent first C/NOFS observation of the storm and the sub-axis is in 2 h intervals. Figure 2e shows the corrected geomagnetic latitudes (via IGRF) in black, the solar local times in blue, and the geographic latitude of the satellite perigees in red.

events examined here, the first three have been considered by *Earle et al*. [2013]. In that work, the storm time neutral density perturbations are compared with observations made from the ground and their magnitudes were shown to be consistent with modeled neutral temperature increases due to energy inputs from high latitudes. Here, we consider the behavior of observed meridional wind perturbations and their relationships to the expected behavior of the high-latitude energy inputs as well as establishing the relationships between the observed neutral density perturbations and the neutral temperature inferred from simultaneous measurements of the ion temperature. In all cases, the angle between the horizontal cross-track direction and the geographic meridian varies around the orbit, being 13° (the orbit inclination) at the equator and 0° at the latitudes extremes of the orbit. All the data examined in this paper are taken at locations away from the geographic equator. Thus, the contribution of a zonal wind component to the horizontal wind component is always less than 20% of the expected meridional wind. The ion temperature is measured from the retarding potential analyzer (RPA) in the IVM [*Heelis and Hanson*, 1998]. These neutral and ion parameters are typically determined along the satellite track with a 2 Hz sample rate. For our purposes, the data are first smoothed using a running median filter with an outer scale of 350 km along the satellite track before the median values and standard deviations of the data for each pass below 410 km are displayed.

[9] Shown in Figure 2a are the hourly averaged values of the solar wind dynamic pressure (SWP) in blue on the right-hand scale, the north-south (Bz) component of the IMF in red on the right-hand scale and the Dst index in black on the left-hand scale over a period of 8 days including a storm that occupied the period from 6 August through 8 August 2011. These data serve as representations of the solar wind drivers and the magnetospheric response. Shown in Figure 2b is a measure of the neutral number density perturbation observed by the CTS that is part of the CINDI instrumentation. This perturbation is represented by the fractional deviation in the sensor pressure at each perigee from a 4 day running average of the measured pressure at perigee. It should be emphasized that the original measurement is of the neutral ram pressure in a chamber, which is in thermal contact with the spacecraft and not significantly sensitive to the ambient neutral gas temperature *Hanson et al*. [1992]. Thus, it is predominantly a measure of the neutral number density.

[10] Figure 2c shows the ion temperature at perigee, as measured by the RPA, and Figure 2d shows the deviation in the neutral gas arrival angle measured by the CTS, as a departure from a 4 day running average of the arrival angle at perigee. The scale to the right of Figure 2d provides a conversion from angle to wind speed assuming a relative satellite velocity of 7.3 kms^{-1}. Figure 2e shows the corrected geomagnetic latitudes (via IGRF) in black on the left-hand scale and solar local times in blue and geographic latitudes in red on the right-hand scale at the locations of the satellite perigees.

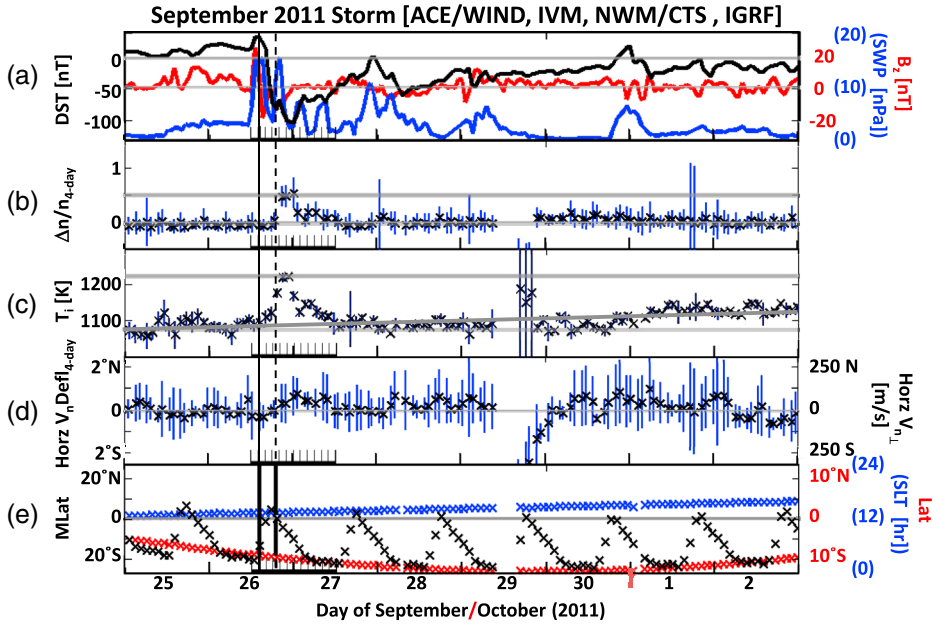

Figure 3. (a–e) September 2011 storm time responses in the upper thermosphere near the magnetic equator. The format is the same as that of Figure 2.

[11] Perigee rotates around the orbit while the orbit plane slowly precesses in local time. Thus, during the 8 day period shown, the local time of perigee changes by less than +3 h and the location of perigee changes in geographic latitude by 5 to 10°. The temporal resolution provided by these data is 96 min (the orbital period); and in addition, each perigee pass lags the previous pass in longitude by about 24°. A solid vertical line is drawn through all panels to denote the approximate storm onset, a dashed line is drawn to denote when C/NOFS observes the event, and a smaller time segment with 2 h intervals surrounds this location at the bottom of each panel to provide some estimate of the timing and duration of the observed perturbations.

[12] In Figure 2, observations are made near the southernmost latitudes of the satellite orbit at 11°S geographic latitude and near 1800 local time. A rapid increase in the solar wind pressure accompanied by a southward turning of the *z* component of the IMF marks the onset of the storm drivers near 2000 UT on 5 August. The Dst responds by reaching a local minimum near −100 nT approximately 3 h later.

[13] At this time, an equatorward perturbation in the meridional wind is seen with an amplitude of about 100 ms^{-1} with a duration of 10–12 h in universal time spanning the longitude region from near 300° to near 180°. At the storm onset, the magnetic South Pole is located in the pre-dawn sector. As the storm progresses, the satellite perigee, which is initially located near the magnetic equator, moves to successively higher magnetic latitudes in the southern hemisphere and the magnetic south pole moves toward local noon. We thus expect the influence of energy inputs from the southern hemisphere is maintained throughout the event.

[14] The thermospheric response at the equator is additionally marked by an increase in the neutral number density by a factor of 1.6, which remains in place for a period of about 15 h before decaying to the background in the following 5 h. Almost colocated with the storm growth phase is a rise in the ion temperature. At this local time, the ion temperature may also be responsive to changes in the ion number density and to plasma transport processes. Generally speaking, there may exist, in this storm and others, additional short-timescale variations in the ion and neutral temperatures associated with solar flares that may sometimes coexist with the longer duration geomagnetic storm perturbations. Thus, the variability in the ion temperature may not always represent a similar variability in the neutral gas temperature. Superimposed on the short-scale variability, however, is a larger time-scale decrease in the temperature indicated by the heavy solid line; and we note that during the storm period, the ion temperature is elevated by 50 to 100 K above this baseline.

[15] A similar storm occurred in the period 25 September–1 October 2011, and is shown in Figure 3. Again, the solar wind drivers and magnetospheric response are shown in Figure 3a; and a measure of the neutral number density perturbation, the ion temperature and the meridional wind perturbation are shown in Figures 3b–3d, respectively, using the same format as in Figure 2. In this case, observations are made at the southern extremes of the orbit, near 11°S geographic latitude at local noon. The solar wind drivers produce a slightly longer growth phase for the storm beginning near 1500 UT on 26 September. The Dst responds by reaching a minimum near −100 nT approximately 7 h later. The southern magnetic pole sweeps across the midnight sector during this period. The north-south component of the IMF suggests that the electromagnetic energy inputs are terminated rather rapidly at the end of the growth phase.

[16] Examination of the meridional wind perturbation shows no signal that can be uniquely identified as a storm response. Some evidence for a small equatorward wind perturbation is suggested but it is comparable to similar perturbations that are not obviously correlated with the solar wind parameters that we have examined. Recall that in this case, the observations are made near the magnetic equator

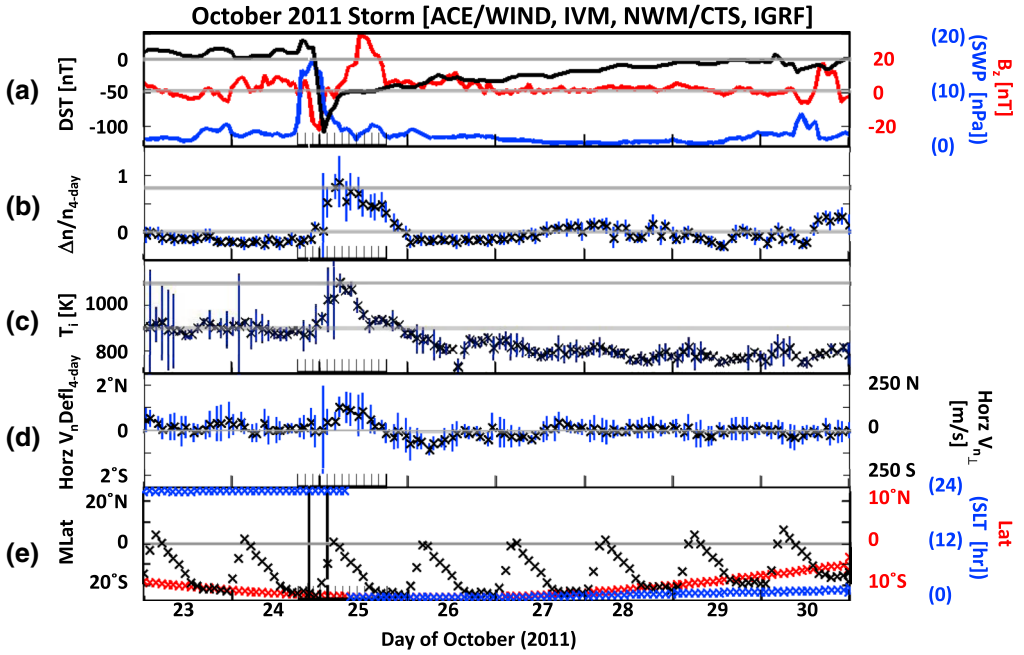

Figure 4. (a–e). October 2011 storm time responses in the upper thermosphere near the magnetic equator. The format is the same as that of Figure 2.

at local noon where winds propagating away from the high latitudes will be opposed by winds blowing away from the sub-solar point near the equator. Thus, a minimum response might be expected for such an observing configuration. Despite the absence of a meridional wind perturbation, a neutral density perturbation is observed about 5 h after the storm onset near 260° longitude. There appear to be two components to the pressure perturbation. Fundamentally, we observe a small increase of about 1.25 beginning during the growth phase and extends about 15 h, in a manner similar to that previously observed. In addition, also beginning during the growth phase, a larger perturbation rising to a magnitude of about 1.5 with duration of about 4 h is observed followed by a rapid decline to the background in a period less than 3 h. Examination of the ion temperature in Figure 3c shows an envelope with similar characteristics to that seen in the perturbation density. Specifically, there is a more extended period over which the ion temperature is elevated by about 50 K and a more limited period in which the ion temperature rises another 100 K.

[17] Figure 4 shows the observed responses in the equatorial thermosphere for the period 23 October–30 October 2011. The figure shows the storm drivers, the magnetospheric response and the thermospheric and ionospheric responses in the same format as Figures 2 and 3. Again, the storm onset is marked by an increase in the solar wind dynamic pressure and a southward turning of the IMF at 2100 UT on 24 October. As before, the storm growth phase marks a rapid decrease in the Dst index to −100 nT in a period of about 4 h. However, the equatorial response is observed at perigee located in the southern hemisphere at 12°S geographic latitude near local midnight; and in this case, a clear equatorward meridional wind perturbation approaching 100 ms^{-1} is observed. The meridional wind rises in about 3 h, and then the perturbation decays over the following 7 h.

[18] We expect that perturbations propagating from high latitudes would be optimally observed near midnight since the poleward flows would be reinforced by day to night flows produced by solar heating. In this case, the observations are initially made in the southern magnetic hemisphere but move toward the magnetic equator as the storm progresses. The southern magnetic pole rotates through the dawn sector toward noon during the storm. Thus, the meridional wind perturbation remains equatorward (northward) throughout the event but not as large as might be expected if the South Pole were to rotate through the midnight sector. During the storm recovery phase after the initial C/NOFS perturbation observations, the north magnetic pole rotates through the midnight sector and the observation location moves toward the magnetic equator. At the end of this period from about 2200 UT on 25 October to about 1200 UT on 26 October, there is some evidence for observation of southward winds indicating that the disturbance originating from the North Pole has reached the observation location.

[19] During this event, the neutral density rises sharply by almost a factor of 2. The subsequent decay of the neutral density perturbation occurs almost linearly over a period of about 15 h spanning the longitude range from 360° to 135°. During this period, we may more confidently identify variations in the ion temperature with variations in the neutral temperature since the thermal contact between the two species is very good and no significant heating of the ions is expected at this post-midnight local time. The temperature shows a slow decline over the entire time period, consistent with the change in local time from near midnight during the storm to 0400 h by 30 October. Superimposed on this slowly declining baseline, shown by the solid line, is an enhancement in the temperature of about 50 K and a temperature perturbation of an additional 200 K occupying the first 10 h from storm onset.

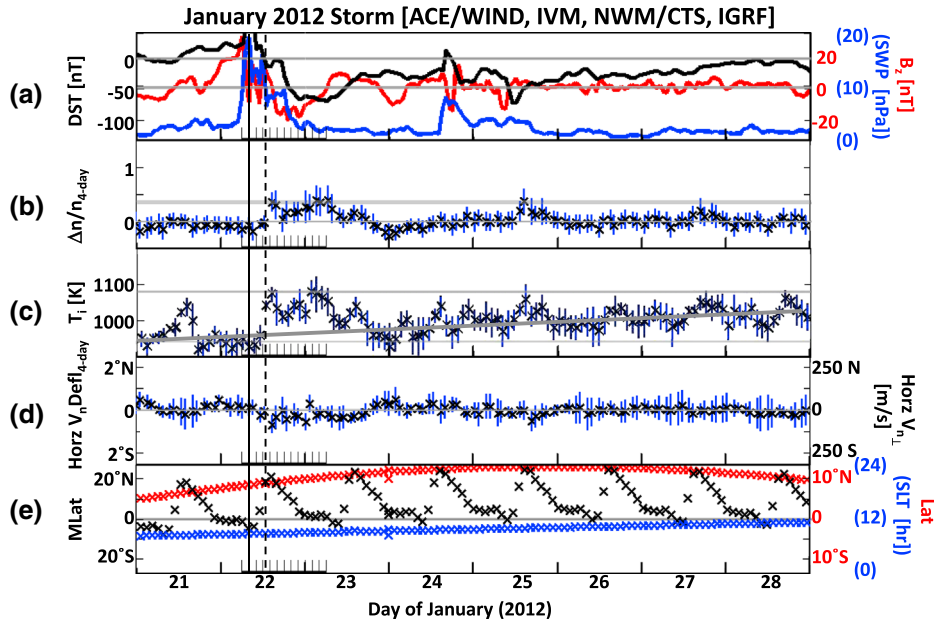

Figure 5. (a–e) January 2012 storm time responses in the upper thermosphere near the magnetic equator. The format is the same as that of Figure 2.

[20] Figure 5 shows the observed responses in the equatorial thermosphere for the storm in January 2012. The presentation format is the same as that shown in the previous figures. Here the change in the Dst index associated with changes in the solar wind drivers is less abrupt in time and smaller in magnitude. It occurs over a period of nearly 20 h beginning near 0800 UT on 22 January. Observations are made at 10°N near 0900 LT in a longitude sector where the satellite is north of the geomagnetic equator and the southern magnetic pole rotates through the afternoon sector toward midnight. No detectable perturbation in the meridional neutral wind is observed or expected under these daytime conditions. However, a significant perturbation in the neutral density is seen throughout the event. Particularly striking in this event is the correlation between changes in the neutral density perturbation and changes in the ion temperature. At this local time, the ion temperature is not expected to match the neutral temperature. However, we might expect that changes in the temperature are associated with changes in the ion cooling-rate, which is dependent on the neutral temperature.

[21] In March 2012, storm responses are observed in the midnight sector at perigee. Figure 6 shows data from a

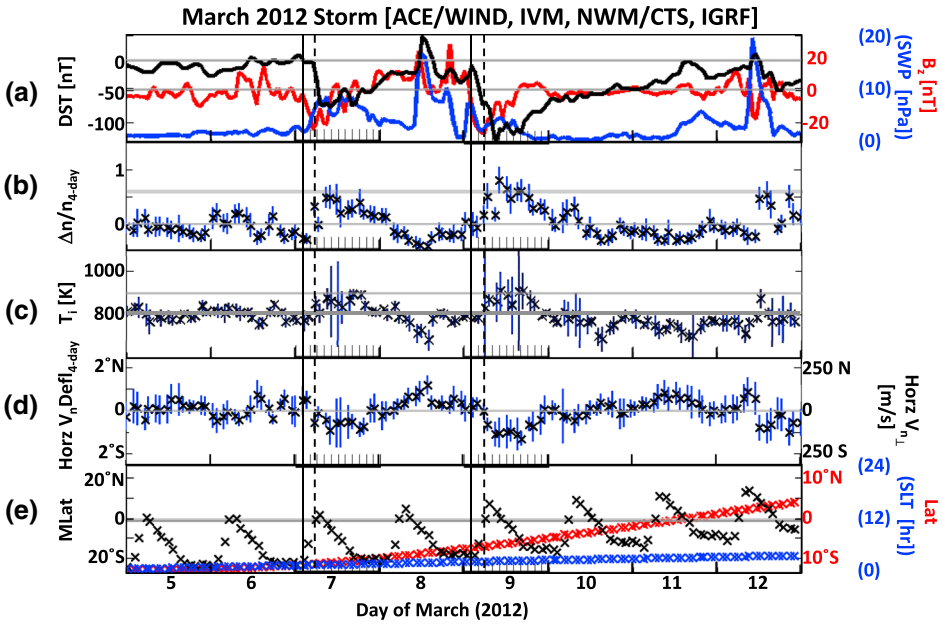

Figure 6. (a–e) March 2012 storm time response in the upper thermosphere neat the magnetic equator. The format is the same as that of Figure 2.

sequence of perigee passes in the period from 5 March to 12 March when two storms occurred associated with southward turnings of the IMF. The solar wind parameters, the Dst index and the response of the topside equatorial ionosphere and thermosphere are shown in the same format as the previous figures. Here, observations are made in the southern hemisphere near 10°S and near 5°S geographic latitude at the geomagnetic equator. Both storm onsets occur near 0200 UT with the Dst reaching a minimum about 4 h later of about −80 nT for the first event and near −120 nT for the second. In this case, a meridional neutral wind surge of near 50 ms^{-1} in the first case and 100 ms^{-1} in the second case is toward the south (poleward) even though the observations are taken near the magnetic equator in the southern hemisphere. However, of most significance here is that the northern magnetic pole rotates through midnight during each of the storms. This would suggest that, in this case, the equatorial neutral thermosphere responds first to the energy inputs in the northern hemisphere. We note that indeed the observations are taken in the magnetic meridian for which the northern magnetic pole is tilted toward the observation point and is located in the nightside where the prevailing day to night motions would reinforce the propagation of disturbances from the high latitude region. This circumstance is also highlighted in the work of *Fuller-Rowell et al*. [1994] showing that, in this meridian plane, the wind surge from the north may cross the geographic equator and remains significant 7 to 12 h after the storm onset.

[22] The strong correlation between neutral density perturbations, ion (and neutral) temperature deviations, meridional neutral wind surges, and the storm onsets are clearly seen in this sequence. Between the storms, there are additional responses related to an increase in the solar wind dynamic pressure, which will not be discussed here. The storm onsets again mark increases in the neutral density at the equator and strong evidence from the ion temperature that the neutral temperature is increased by about 50 K in the first event and by about 80 K in the second.

3. Discussion

[23] The observations shown here are remarkably consistent with previous modeling studies, although neither the external drivers nor the observational configurations are reproduced in a precise way in the reported model results [*Fuller-Rowell et al*., 1994, *Lu et al*., 2012]. For these observations, each storm response is recorded near the magnetic equator at a relatively fixed local time over a wide range of longitudes. Thus, the previously reported storm time longitude variations [*Fuller-Rowell et al*., 1994] are convolved with the universal time progressions that are seen. The five storm events studied here are insufficient to provide a systematic description of local time and longitude variations at the equator. However, in all cases, we see that solar wind drivers include a southward turning of the IMF and produce a reduction in the Dst index to levels near −100 nT, and there are a number of basic principles revealed in model results that are consistent with the findings here.

[24] When examining the accompanying perturbations in the meridional neutral wind, we find that the response is highly dependent upon the local time, the longitude of the observation and the universal time of the storm onset, which determines the location of the magnetic poles with respect to the noon–midnight meridian. The model results from *Fuller-Rowell et al*. [1994] suggest that the most significant meridional wind perturbations will be seen in the evening and midnight sectors as is observed here. We find that while storm time perturbations in the density and temperature are systematically seen on the dayside and the nightside in the upper thermosphere, significant meridional wind perturbations are only seen in the evening and midnight sectors. This appears consistent with the suggestion that on the dayside, the storm winds compete with the usual prevailing poleward circulation. However, at night, the two wind systems constructively support equatorward motion and thus generate stronger wind responses [*Fuller-Rowell et al*. 1994]. It has been further suggested by *Fuller-Rowell et al*. [1994] that the largest perturbations will be seen for storms that occur while the magnetic pole is rotating through the midnight sector and that under these conditions the perturbed atmosphere may propagate from that polar region across the magnetic equator.

[25] We have demonstrated two cases when this condition largely prevails. One case occurs in October 2011, where the southern magnetic pole is in the midnight sector at storm onset, and the observations are made near midnight at 10°S geographic latitude in the southern magnetic hemisphere. In this case, an equatorward (northward) wind perturbation of roughly 100 ms^{-1} is observed 4 to 5 h after the storm onset. This observation taken at the southern extreme of the orbit can be unambiguously identified as a meridional wind perturbation associated with the expanding influence of energy inputs in the southern hemisphere. Another case occurs in March 2012 when the northern magnetic pole is in the midnight sector, and observations are made near midnight and between 5°S and 10°S geographic latitude and spanning the magnetic equator. In this case, the North Pole is in the nighttime sector and a southward wind perturbation of order 100 ms^{-1} is observed 4 to 5 h after the storm onset. Here a westward zonal wind perturbation, which *Fuller-Rowell et al*. [1994] suggests, will be less than 100 ms^{-1}, could contribute at most 20% of the signal that we attribute to a meridional wind perturbation. However, the direction of the meridional wind perturbation cannot be changed. It is directed away from the North Polar Region in agreement with the expectation that in this longitude sector, the energy inputs at northern high latitudes will dominate the dynamics at the equator near midnight.

[26] Significant meridional wind perturbations during the August 2011 storm are also seen near 1800 local time, consistent with the equatorial expansion of a newly heated atmosphere at higher latitudes and a rotation to the west to conserve angular momentum. For this simple case, the wind perturbation conforms to the expectation that an equatorward perturbation will be observed originating from energy inputs in the polar region of the hemisphere in which the observation is made (in the southern hemisphere, for this case).

[27] For the events studied here, the zonal wind is not recovered by the NWM and the influence of the zonal wind perturbation on the horizontal wind shown here is very small. Thus, direct evidence for storm time modification of the zonal wind, which is expected to be ~100 m/s westwards, cannot be presented. On the dayside, significant storm time meridional wind perturbations are not observed. Whether

this is due to dominance of zonal flows across the dayside or the fact that the high latitude disturbance does not propagate to the equator cannot be unambiguously addressed.

[28] In each of the events, there is strong evidence that the neutral atmospheric temperature becomes elevated at the equator by 50 to 150 K. Although in this study we do not have a direct measure of the neutral temperature, we have made direct measurements of associated ion temperatures near an altitude of 400 km. During the nighttime, we have measured an ion temperature near 800 K and assume that the thermal contact between the ions and neutrals makes the ion temperature a good proxy for the neutral temperature [*Heelis et al*., 2009]. During the daytime, we assume that the changes in the ion temperature are only produced by changes in the ion cooling-rate and therefore also represent changes in the neutral temperature. The estimates of neutral temperature variations implied in this way are consistent with those derived from a model as reported by *Earle et al*. [2013]. Elevated temperatures in the thermosphere during the storm exist behind a phase front that propagates toward the equator at 400–800 ms^{-1} and arrives in the equatorial region some 3–5 h after the southward turning of the IMF. As mentioned previously, there are no significant changes in the neutral wind associated with the dayside in situ storm observations at an altitude of 400 km. Thus, we assume that heat is transferred by conduction to the lowest latitudes allowing the density and temperature enhancement perturbations to be readily observed. Such conduction is discussed in detail at high latitudes by *Huang et al*. [2012]. If we assume that the heating rates that produce the elevated neutral temperature are imposed above 180 km altitude [*Fuller-Rowell*, 1995; *Thayer and Semeter*, 2004] and that the newly heated atmosphere is in hydrostatic equilibrium by the time it reaches the equator, then the increase in the neutral scale height would produce a fractional increase in the neutral number density at an altitude near 400 km between 0.3 and 1.0. This range is well represented by the observed changes in neutral number density. However, changes in the mean mass of the atmosphere as appear in the model of *Fuller-Rowell et al*. [1994] can introduce additional variability into the relationship between the density and temperature perturbations. For the fall 2011 storms, *Earle et al*. [2013] find a similar agreement between the neutral density perturbations and the thermospheric temperatures measured by a ground-based system in South America. A temperature increase of about 150 K at 0900 solar local time observed on 21 January is most likely due to Coulomb collisions with electrons at elevated temperatures, usually expected post-sunrise [*Bhuyan et al*., 2004; *Pavlov et al*., 2001]. One should note that there are no appreciable increases in the neutral density at this time because the increase in ion temperature is due to Coulomb collisions, not ion cooling-rate changes.

[29] It should also be noted that portions of the storm events in September 2011 and January and March 2012 are coincident with solar flares, which may produce additional enhancements in the ionosphere and thermosphere [*Qian et al*., 2011]. However, the events in August and October 2011 discussed in this paper do not coincide with flares on the timescales of interest (within one orbit, or about 96 min), and the largest changes in all of the five events are clearly due to the geomagnetic inputs. Further discussion about the separation of solar and geomagnetic effects can be found in *Qian et al*. [2011].

4. Conclusions

[30] Storm time energy inputs at high latitudes produce modifications to the upper thermosphere that propagate to the equatorial regions within a few hours. These perturbations in the neutral temperature, density, and circulation are observed near 400 km altitude by the CINDI instrumentation flying aboard the C/NOFS satellite. Perturbations in the neutral density are observed directly and are consistent with a change in the neutral scale height associated with an elevated neutral temperature that can be deduced from direct measurements of the ion temperature near 400 km altitude. Perturbations of the meridional neutral wind are also observed but are restricted to the evening and midnight sectors. These observations, which are biased to the southern side of the magnetic equator, are dominated by energy inputs at southern high latitudes except in one case when the northern magnetic pole rotates through midnight during the storm onset. In this case, the energy inputs from northern high latitudes influence the meridional flow.

[31] **Acknowledgments.** This work is supported by NASA grant NNX10AT02G to the University of Texas at Dallas.

[32] Robert Lysak thanks the reviewers for their assistance in evaluating this paper.

References

Bhuyan, P. K., M. Chamua, P. Subrahmanyam, and S. C. Garg (2004), Diurnal, seasonal and latitudinal variations of ion temperature measured by the SROSS C2 satellite in the Indian zone equatorial and low latitude ionosphere and comparison with the IRI, *J. Atmos. Sol. Terr. Phys.*, *66*(3–4), 301–312, doi:10.1016/ j.jastp.2003.12.002.

Burton, R. K., R. L. McPherron, and C. T. Russell (1975), An empirical relationship between interplanetary conditions and Dst, *J. Geophys. Res.*, *80*(31), 4204–4214.

Earle, G. D., R. L. Davidson, R. A. Heelis, W. R. Coley, D. R. Weimer, A. J. Gerrard, J. J. Makela, and J. Meriwether (2013), Low latitude thermospheric responses to magnetic storms, *J. Geophys. Res.*, *118*, doi:10.1002/jgra.50212, in press.

Emery, B. A., C. Lathuillere, P. G. Richards, R. G. Roble, M. J. Buonsanto, D. J. Knipp, P. Wilkinson, D. P. Sipler, and R. Niciejewski (1999), Time dependent thermospheric neutral response to the 2–11 November 1993 storm period, *J. Atmos. Sol. Terr. Phys.*, *61*, 329–350.

Emmert, J. T., B. G. Fejer, C. G. Fesen, G. G. Shepherd, and B. H. Solheim (2001), Climatology of middle- and low-latitude daytime F region disturbance neutral winds measured by Wind Imaging Interferometer (WINDII), *J. Geophys. Res.*, *106*(A11), 24,701–24,712, doi:10.1029/ 2000JA000372.

Fejer, B. G., J. T. Emmert, G. G. Shepherd, and B. H. Solheim (2000), Average daytime F region disturbance neutral winds measured by UARS: Initial results, *Geophys. Res. Lett.*, *27*(13), 1859–1862, doi:10.1029/ 2000GL003787.

Forbes, J. M., R. Gonzalez, F. A. Marcos, D. Revelle, and H. Parish (1996), Magnetic storm response of lower thermosphere density, *J. Geophys. Res.*, *101*(A2), 2313–2319, doi:10.1029/95JA02721.

Fuller-Rowell, T. J. (1995), The dynamics of the lower thermosphere, in *The Upper Mesosphere and Lower Thermosphere: A Review of Experiment and Theory*, Geophys. Monogr. Ser., vol. *87*, edited by R. M. Johnson and T. L. Killeen, pp. 23–36, AGU, Washington, D. C., doi:10.1029/GM087p0023.

Fuller-Rowell, T. J., M. V. Codrescu, R. J. Moffett, and S. Quegan (1994), Response of the thermosphere and ionosphere to geomagnetic storms, *J. Geophys. Res.*, *99*(A3), 3893–3914, doi:10.1029/93JA02015.

Fuller-Rowell, T. J., G. H. Millward, A. D. Richmond, and M. V. Codrescu (2002), Storm-time changes in the upper atmosphere at low latitudes, *J. Atmos. Sol. Terr. Phys.*, *64*, 1383–1391.

Gardner, L. C., and R. W. Schunk (2010), Generation of traveling atmospheric disturbances during pulsating geomagnetic storms, *J. Geophys. Res.*, *115*, A08314, doi:10.1029/2009JA015129.

Haaser, R. A., G. D. Earle, R. A. Heelis, W. R. Coley, and J. H. Klenzing (2010), Low-latitude measurements of neutral thermospheric helium dominance near 400 km during extreme solar minimum, *J. Geophys. Res.*, *115*, A11318, doi:10.1029/2010JA015325.

Hanson, W. B., U. Ponzi, C. Arduini, and M. DiRuscio (1992), A satellite anemometer, *J. Astro. Sci.*, *40*, 429.

Heelis, R. A., and W. B. Hanson (1998), Measurements of Thermal Ion Drift Velocity and Temperature Using Planar Sensors, *Measurement Techniques in Space Plasmas: Particles, Geophys. Monogr. Ser.*, *102*, *AGU*, 61.

Heelis, R. A., W. R. Coley, A. G. Burrell, M. R. Hairston, G. D. Earle, M. D. Perdue, R. A. Power, L. L. Harmon, B. J. Holt, and C. R. Lippincott (2009), Behavior of the O+/H + transition height during the extreme solar minimum of 2008, *Geophys. Res. Lett.*, *36*, L00C03, doi:10.1029/2009GL038652.

Huang, Y., A. D. Richmond, Y. Deng, and R. G. Roble (2012), Height distribution of Joule heating and its influence on the thermosphere, *J. Geophys. Res.*, *117*, A08334, doi:10.1029/2012JA017885.

International Association of Geomagnetism and Aeronomy, Working Group V-MOD (2010), International geomagnetic reference field: The eleventh generation, *Geophys. J. Int.*, *183*, 1216–1230, doi:10.1111/ j.1365-246X.2010.04804.x.

Lu, G., L. Goncharenko, M. J. Nicolls, A. Maute, A. Coster, and L. J. Paxton (2012), Ionospheric and thermospheric variations associated with prompt penetration electric fields, *J. Geophys. Res.*, *117*, A08312, doi:10.1029/2012JA017769.

Lühr, H., J. Park, P. Ritter, and H. Liu (2012), In-situ CHAMP observations of ionosphere-thermosphere coupling, *Space Sci. Rev.*, *168*, 230–260, doi:10.1007/ s11214-011-9798-4.

Martinis, C., J. Meriwether, R. Niciejewski, M. Biondi, C. Fesen, and M. Mendillo (2001), Zonal neutral winds at equatorial and low latitudes, *J. Atmos. Sol. Terr. Phys.*, *63*, 1559–1569, doi:10.1016/S1364-6826(01) 00022-0.

Pavlov, A. V., T. Abe, and K.-I. Oyama (2001), Comparison of the measured and modeled electron densities and temperatures in the ionosphere and plasmasphere during the period 25–29 June 1990, *J. Atmos. Sol. Terr. Phys.*, *63*(6), 605–616.

Qian, L., A. G. Burns, P. C. Chamberlin, and S. C. Solomon (2011), Variability of thermosphere and ionosphere responses to solar flares, *J. Geophys. Res.*, *116*, A10309, doi:10.1029/2011JA016777.

von Rosenvinge, T. T., et al. (1995), The energetic particles: Acceleration, Composition, and Transport (EPACT) experiment on the WIND spacecraft, *Space Sci. Rev.*, *71*, 155.

Saiz, E., C. Cid, and Y. Cerrato (2008), Forecasting intense geomagnetic activity using interplanetary magnetic field data, *Ann. Geophys.*, *26*, 3989–3998.

Shepherd, G. G., et al. (1993), WINDII, the wind imaging interferometer on the upper atmosphere research satellite, *J. Geophys. Res.*, *98*(D6), 10,725–10,750, doi:10.1029/93JD00227.

Stone, E. C., A. M. Frandsen, R. A. Mewaldt, E. R. Christian, D. Margolies, J. F. Ormes, and F. Snow (1998), The advanced composition explorer, *Space Sci. Rev.*, *86*, 1–22, doi:10.1023/A:1005082526237.

Sutton, E. K., J. M. Forbes, and R. S. Nerem (2005), Global thermospheric neutral density and wind response to the severe 2003 geomagnetic storms from CHAMP accelerometer data, *J. Geophys. Res.*, *110*, A09S40, doi:10.1029/2004JA010985.

Thayer, J. P., and J. Semeter (2004), The convergence of magnetospheric energy flux in the polar atmosphere, *J. Atmos. Sol. Terr. Phys.*, *66*, 807–824.

Weimer, D. R., B. R. Bowman, E. K. Sutton, and W. K. Tobiska (2011), Predicting global average thermospheric temperature changes resulting from auroral heating, *J. Geophys. Res.*, *116*, A01312, doi:10.1029/ 2010JA015685.

Wu, Q., T. L. Killeen, and N. W. Spencer (1994), Dynamics Explorer 2 observations of equatorial thermospheric winds and temperatures: Local time and longitudinal dependences, *J. Geophys. Res.*, *99*(A4), 6277–6288, doi:10.1029/93JA02521.